

# 01.01 Introduction to GW Science

## GW Foundations

Perturbations of the flat spacetime metric about a background:

$$g_{\mu\nu} = \eta_{\mu\nu} + h_{\mu\nu}$$

where  $h_{\mu\nu} = A_{\mu\nu} \exp(i2\pi ft)$  is the transverse traceless tensor, with two polarizations (independent degrees of freedom).

## Detectors

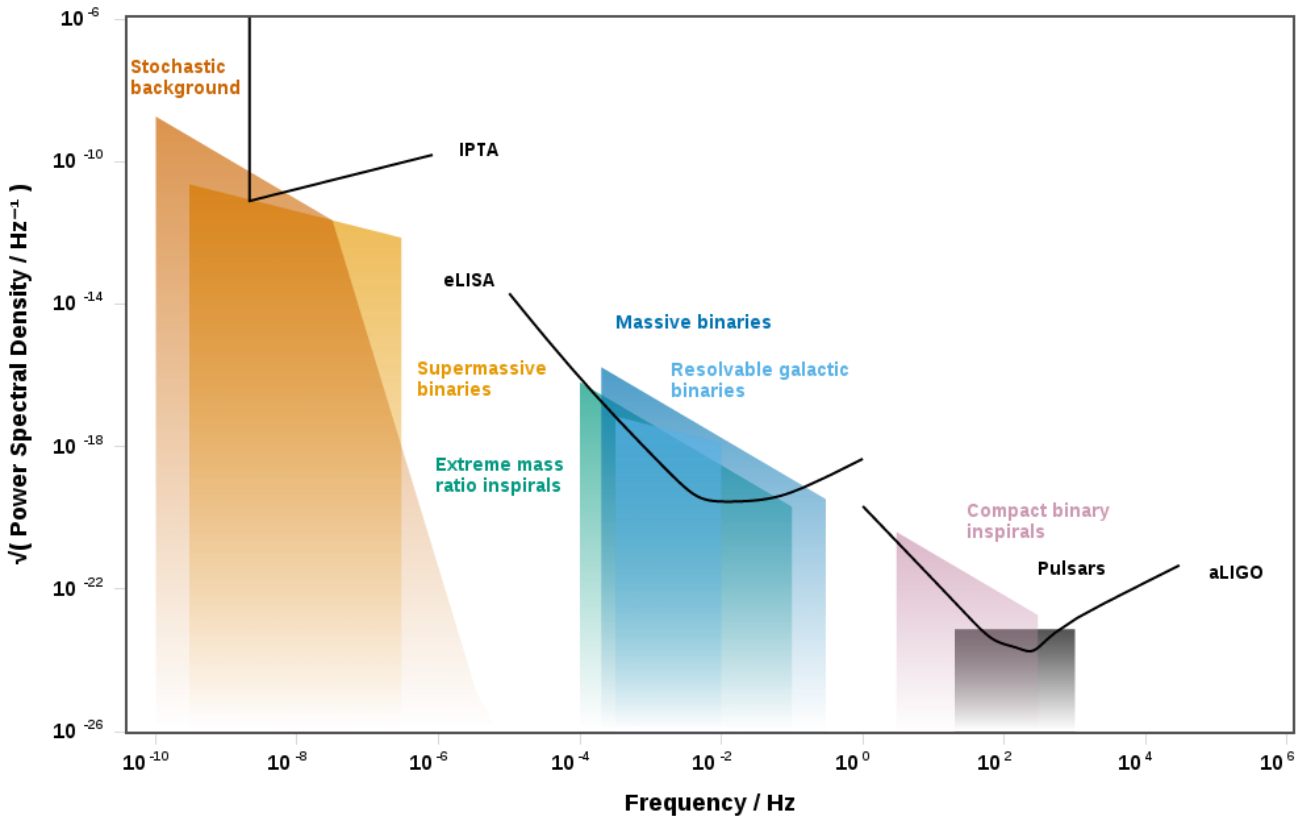
Weber's Bar Detector: Giant metal chunk with strain gauges. Sensitive to resonant frequencies, narrow sensitivity.

 **Comeback! >**

The Moon is a resonant sphere!

Michelson Interferometer: Freely-falling masses. Sensitive to mechanical frequencies.

LIGO: Fabry-Perot cavities, with Michelson Interferometers. 4km Fabry-Perot cavity. Scales the metric perturbations  $h = \frac{\Delta L}{L}$ . Also aids coherence by the frequency as the inverse of the time period between end points. Effective length  $\sim 10^6$  m, effective 300 Hz. Noise cutoffs.



Multiple detectors help in *triangulation*, through relative delays in arrival time on the detector. Single detector analysis results in overall sky location with maxima and minima dependent on detector characteristics. Sky location through two detectors characterized by a ring (hyperbola) on the celestial sphere. Highly constrained sky localization on all three detectors.

## Sources

Source Morphology:

- Anything with a changing mass asymmetry
- Binary Black Holes/ Neutron Stars  $h \sim \mathcal{O}(10^{-21})$  with  $f \sim \mathcal{O}(10^2)$  Hz
- Strongest sources are *heavy and move quickly*: compact BBH, BNS, NSBH.
- Other compact sources: Spinning quadropolar neutron stars, Supernova explosions, Hyperbolic encounters, Astrophysical foreground due to CBCs

Binary formation channels:

- Isolated evolution
- Dynamical Capture in dense clusters
- Active Galactic Nuclei assisted mergers

## Waveforms

<https://arxiv.org/abs/gr-qc/0211028>

$$h_+ = A_+(t) \exp(\iota 2\pi f_+(t)t)$$

$$h_\times = A_\times(t) \exp(\iota 2\pi f_\times(t)t)$$

Assume circular orbit and quadroplar moment of inertia tensor

$$I_{(0)} \sim \mu R^2 \exp(\iota \Omega t)$$

The strain is thereby

$$h_{(0)} \sim \frac{2G\ddot{I}_{(0)}}{c^4 d}$$

where we take the *retarded* time  $t - \frac{d}{c}$ . Further assuming Keplerian orbits, we take  $\Omega^2 = \frac{GM}{R^3}$ , thereby we have

$$h_{(0)} \sim \frac{4G^2}{c^4} \frac{1}{d} \frac{\mu M}{R}$$

The luminosity, given by the loss in energy is

$$L_{GW} = -dE/dt = 4\pi d^2 |\dot{h}_{(0)}|^2 \sim \frac{64\pi G^4}{c^8} \frac{\mu^2 M^2}{R^4} \left( \frac{dR}{dT} \right)^2$$

Loss of circular orbit, by reducing the radial separation, can be found from the gravitational potential change  $V = -\frac{GM}{R}$  and  $\frac{dE}{dR} = \frac{dV}{dR}$ , thereby we get

$$\frac{dR}{dt} = \frac{\frac{dE}{dt}}{\frac{dE}{dR}} = -\frac{64\pi G^3}{c^8} \frac{\mu^2 M}{R^2} \left( \frac{dR}{dT} \right)^2$$

Thereby, we have

$$\frac{dR}{dt} = -\frac{c^8}{64\pi G^3 \mu^2 M} R^2$$

hence solving,

$$R = - \left( \frac{c^8}{64\pi G^3 \mu^2 M} \right) \frac{1}{(T-t)}$$

Hence, we compute the quadrupole frequency of radiation from the orbital frequency,

$$f_{GW} = 2f_{orb} = \frac{\Omega}{\pi} = \frac{5^{\frac{3}{8}}}{8\pi} \left( \frac{c^3}{G\mathcal{M}} \right)^{\frac{5}{8}} \frac{1}{(T-t)^{\frac{3}{8}}}$$

where  $\mathcal{M} = \mu^{\frac{3}{5}} M^{\frac{2}{5}}$

For accuracy, Post Newtonian expansions, order by order. Numerical Relativity.

Approximation breaks down for late inspiral, when the decay is fast and non quasi circular.

$$\tau = \frac{R}{\frac{dR}{dt}} = P_{orb} = \frac{2}{f_{GW}}$$

Waveforms parameterization:

- Intrinsic parameters:
  - Source masses  $m_1, m_2$
  - Spin Vectors  $\vec{a}_1, \vec{a}_2$
- Extrinsic parameters:
  - Source Orientation (*inclination*)  $\iota$
  - Antenna Patterns (*polarization and phase of coalescence*)  $\psi, \phi$
  - Equatorial Coordinates (*right ascension and declination*)  $\alpha, \delta$
  - Luminosity Distance  $d_L$
  - Consequential alignment of orientation results in maximal coverage in relative parallel directions.

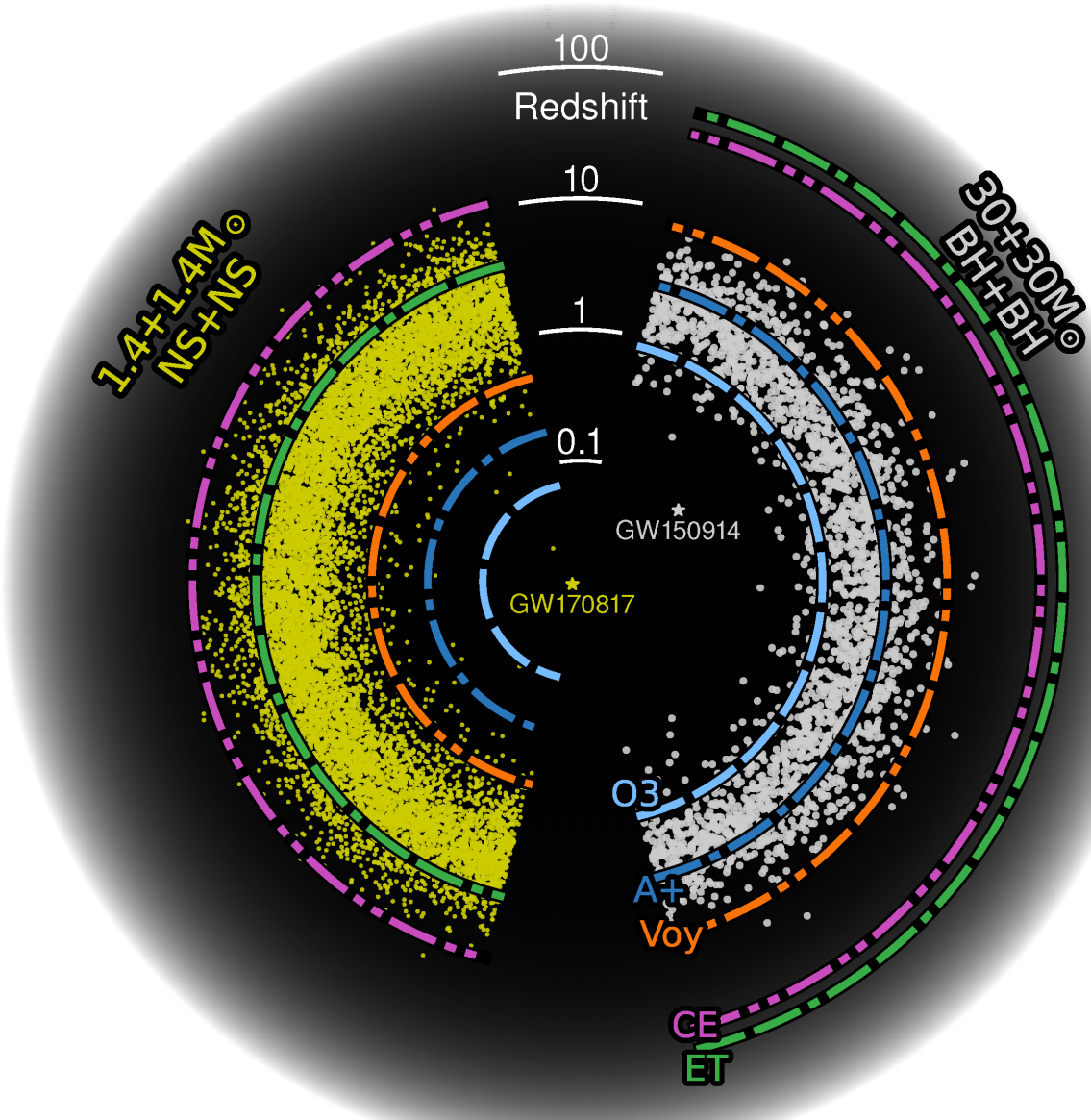
Overall, 15 parameter modelling, with time/frequency, such that

$$h(t/f) = F_+ h_+ + F_\times h_\times$$

## GW Astronomy

- Non attenuation, propagation is free
- May undergo refraction, *gravitational lensing*
- Sensitivity depends on loudness of signal relative to noise

- Detection Range, proportional to distance, dependent on source



- Detection volume higher, larger Detection rates

# 01.02 Introduction to Fourier analysis, Noise Sensitivity

Strain data

$$h(t) = s(t) + n(t)$$

- For Michelson interferometer, we have the strain  $h := \frac{\Delta l}{L} \sim \frac{\lambda_{\text{Laser}}}{l} \sim \mathcal{O}(10^{-9})$
- Fabry-Perot cavity for increasing effective path length  $h \sim \frac{\Delta l}{l_{\text{eff}}} = \frac{\lambda_{\text{Laser}}}{\lambda_{\text{GW}}} \sim \mathcal{O}(10^{-12})$ , since the threshold comes by the wavelength of the GW wave.
- Fraction of fringe-width due to intensity of fluctuations of photons. Photon Poisson statistics,  $\Delta l \sim \frac{\lambda_{\text{Laser}}}{\sqrt{N_{\text{photons}}}}$ , such that the number of photons, collected in one cycle  $N = \frac{P}{\frac{hc}{\lambda_{\text{Laser}}}} \tau_{\text{GW}} = \frac{P}{\frac{hc}{\lambda_{\text{Laser}}}} \frac{1}{f_{\text{GW}}}$ , thereby,  $h \sim \frac{\Delta l}{l_{\text{eff}}} = \frac{\lambda_{\text{Laser}}}{\sqrt{N_{\text{photons}} \lambda_{\text{GW}}}} \sim \mathcal{O}(10^{-20})$ .

## Sampling

Minimum necessary sampling frequency is twice the frequency of the gravitational wave, by the *Nyquist Shannon-Sampling Theorem*, thereby

$$f_s = \frac{1}{\Delta t} = 2f_{\max}$$

since the sampling requires accuracy to prevent aliasing and misinterpretation.

## Fourier Space

Fourier transformation of data,

$$\mathcal{F}(h) := \tilde{h}(f) = \int_{-\infty}^{\infty} h(t) \exp(-i2\pi ft) dt$$

For finite length of signals, we use a window function

$$\omega(t) = \begin{cases} 1 & 0 \leq t \leq T \\ 0 & \text{otherwise} \end{cases}$$

such that  $\mathcal{F}\{g(t)\} = \tilde{g}(f) = (\tilde{h} * \tilde{\omega})(f)$ , hence  $\mathcal{F}\{h(t)\} \neq \tilde{h}(f)$ .

Windowing causes erroneous effects due to *spectral leakage* in the frequency domain, choice of better windows. Special window functions including rectangular, hanning. Gaussian. Attenuates lot of valid data. To incorporate overlapping techniques to minimize data loss through segment.

Note the *Ergodic theorem* Implies

$$\langle h^2 \rangle = \lim_{T \rightarrow \infty} \frac{1}{T} \int_0^T h^2(t) dt$$

Further, the *Parseval's theorem* implies,

$$\langle h^2 \rangle = \lim_{T \rightarrow \infty} \frac{1}{T} \int_0^T h(t) \exp(\iota 2\pi f t) \int_{-\infty}^{\infty} h(t') \exp(-\iota 2\pi f t') dt' = \lim_{T \rightarrow \infty} \frac{1}{T} \int_{-\infty}^{\infty} |\tilde{h}(f)|^2 df$$

We define the *Power Spectral Density* as

$$S_n(f) = \lim_{T \rightarrow \infty} \frac{2}{T} \left| \int_0^T h(t) \exp(-\iota 2\pi f t) dt \right|^2$$

such that

$$\langle h^2 \rangle = \int_0^{\infty} S_n(f) df$$

The power spectral density is reexpressed as

$$S_n(f) = 2 \int_{-\infty}^{\infty} R(\tau) \exp(-\iota 2\pi f \tau) d\tau$$

where the *autocorrelation* function

$$R(\tau) = \lim_{T \rightarrow \infty} \frac{1}{T} \int_0^T h(t) h(t + \tau) dt$$

Thereby, in the frequency domain,

$$\langle \tilde{h}^*(f') \tilde{h}(f) \rangle = \int_{-\infty}^{\infty} h(t) \exp(-\iota 2\pi f t) dt \int_{-\infty}^{\infty} h(t') \exp(-\iota 2\pi f' t') dt'$$

such that, we have

$$\langle \tilde{h}^*(f') \tilde{h}(f) \rangle = \frac{1}{2} S_n(f) \delta(f - f')$$

If  $S_n(f) = S_0$  is constant with  $f$ , white noise, else coloured noise. Welch method used for PSD estimation, for repeated segmentation through windowing. Standard duration and overlap fixed, with Hann windowing.

Assuming wide sense stationery noise, to have

$$\langle n(t) \rangle = \langle n(t + \tau) \rangle$$

with same mean, and same covariance (ergodic random process)

$$C(\tau) = \langle n(t)n(t + \tau) \rangle = \langle n(t')n(t' + \tau) \rangle$$

such that we have the distribution

$$p[n(t)] = \frac{1}{(2\pi)^{\frac{N}{2}} \sqrt{\det C}} \exp\left(-\frac{1}{2} \vec{n}^T C^{-1} \vec{n}\right)$$

where  $C_{ij} = \langle n_i n_j \rangle$ .

There can exist non-Gaussianities, non-stationarities in the data, which cause spurious spectral issues. Segmenting the data can prevent Gibbs effect.

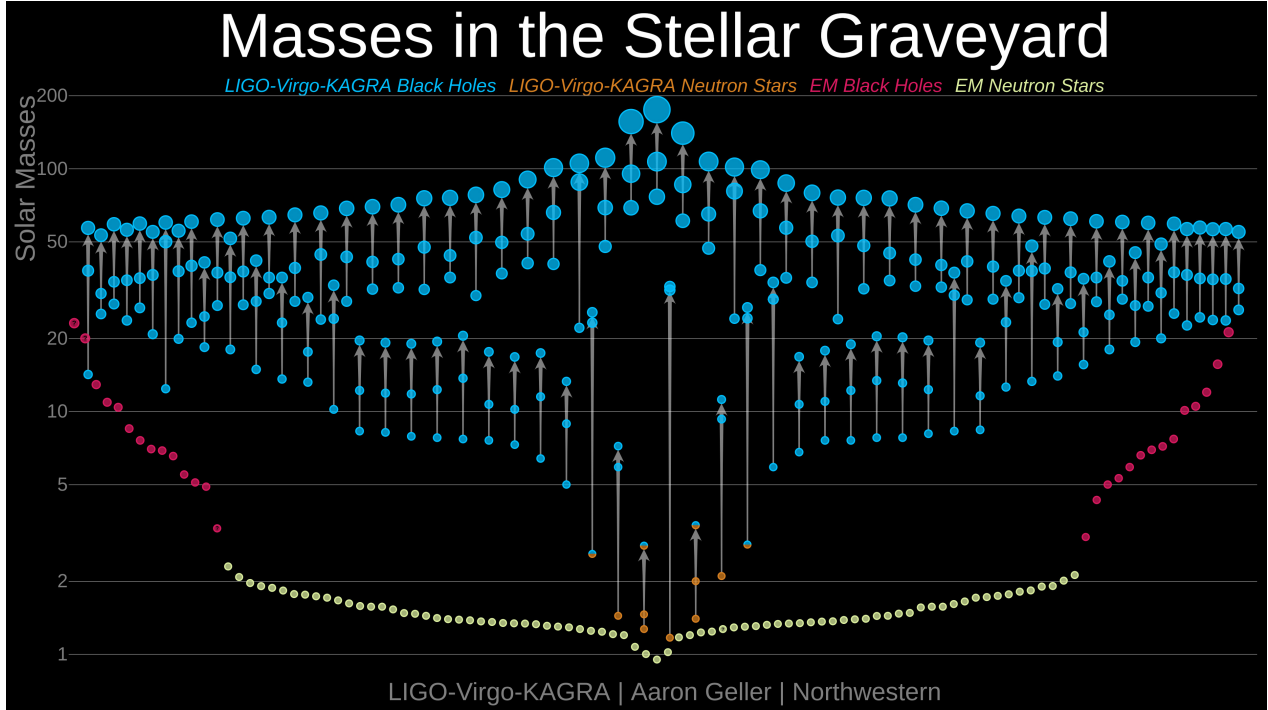
Time frequency analysis proceeded by Spectograms and Q-transforms. Distribution of signal power across time and frequency domains. Uniform tile windows for spectrograms, and variable-sized windows that scale with frequency for Q-transforms, where lower frequencies have longer windows for better frequency resolution through logarithmic tiling. Re-weighting the data with respect to PSD.

$$\tilde{h}(f) \rightarrow \tilde{h}'(f) = \frac{h(f)}{\sqrt{S_n(f)}}$$

## 02.01 Science with CBCs

### Stellar Physics

- Compactness with massive structures  $\mathcal{O}(10 - 100) M_{\odot}$ , fast moving.
- Stellar evolution resulting in heavy mass black holes



- Merger in early age of the universe, accretion disk radiating emission
- Interesting physics of intermediate masses, resulting in a lower mass gap around  $3 - 5 M_{\odot}$ , but events observed. Further upper mass gap around  $60 - 150 M_{\odot}$ . Hierarchical mergers, sequential explanations
- Nuclear equation of state, through neutron star analysis of tidal deformability  $\Lambda$

### Population Studies

- Astrophysical distribution of merger rate as function of primary black hole masses: Peak near  $40 M_{\odot}$ , likely because *pulsational pair instability supernova*, and drop due to *pair instability supernova*.  
Core collapse supernova due to surplus nuclear pressure due to compression and rebounding. Neutron stars due to protons fusing to form, and further collapse.  
Photons pair production  $\gamma \rightarrow e^+ + e^-$ , decrease in pressure and compression, no remnant due to pair instability. If less extreme, pulsational instability, existence in the mass gap. Spin distribution are low spaced, with differential spaced tilts.
- Binary formation channels: *Isolated*, starts with the stellar binary, supernova explosions and mass transfers, envelope expands (*mirror principle*), drag force reduces separation. Expected aligned spins (nearly, due to supernova kicks) and no detectable *eccentricity* due to circularization through GW emission.

*Dynamical*, encounters with stellar clusters, tighter orbits. Expected isotropic spin distribution, and detectable eccentricity.

## Tests of General Relativity

- IMR Consistency Test

$M_f, \chi_f$  inferred from the *inspiral* regime of the signal through the initial masses and spins:  $M_f \equiv M_f(m_1, m_2, \vec{S}_1, \vec{S}_2)$  and  $\chi_f \equiv \chi_f(m_1, m_2, \vec{S}_1, \vec{S}_2)$ , and consistency measured from the *ringdown* regime.  $\Delta M_f/M_f$  and  $\Delta \chi_f/\chi_f$  must be consistent about zero

- Parameterized Tests of GR

Post Newtonian series

$$\varphi_{PN} = 2\pi f t_c - \varphi_c - \frac{\pi}{4} + \frac{3}{128\eta} \frac{1}{(\pi \bar{f})^{\frac{5}{3}}} \sum_{i=-2}^7 [\varphi_i + \varphi_{il} \log(\pi \bar{f})] (\pi \bar{f})^{\frac{i}{3}}$$

Introducing deviations  $\delta\varphi_i$  in the GR coefficients  $\varphi_i$ , as a variable fit. Note that the PN order is given by the coefficient  $\varphi_i$  as  $\frac{1}{2}i$  PN order.

- Black Hole Spectroscopy

Settling into Kerr Black Hole:

$$h_+(t) - i h_\times(t) = \sum_{\ell=2}^{\infty} \sum_{m=-\ell}^{\ell} \sum_{n=0}^{\infty} \mathcal{A}_{\ell mn} \exp\left(-\frac{t-t_0}{(1+z)\tau_{\ell mn}}\right) \exp\left(-i \frac{2\pi f_{\ell mn}}{1+z}(t-t_0)\right) S_{\ell mn}(\theta, \varphi, \chi_f)$$

Note that the damping time  $\tau_{\ell mn}$  and frequency  $f_{\ell mn}$  are uniquely determined from  $M_f$  and  $\chi_f$ . Only dominant mode  $(2, 2, 0)$  detected so far.  $t_0$  non uniquely determined, different values used to understand if posteriors are consistent.

## Cosmological Studies

- Earlier studies through CMB anisotropies, and standard candles (Cepheid variable stars, and Type I Supernova) through intensity measurements and building the distance ladder from redshift  $d(z)$  measurements. Crisis in cosmology.
- Gravitational waves as standard sirens,  $h \propto \frac{1}{d_L}$ , where  $d_L$  is independent of any distance ladder. Inference of  $d_L(z)$ . For bright sirens, redshift  $z$  can be measured from the electromagnetic counterpart. For dark sirens, localization of a galaxy cluster. Estimate of  $H_0$  is obtained.
- Lensing of gravitational waves, time delay distributions. Deflection of gravitational waves by spacetime curvature. Time delay distribution dependent on the lens mass and the impact parameters.

## 02.02 Introduction to Matched Filtering, False Alarm Statistics

### Bayesian Analysis

Null hypothesis  $\mathcal{H}_0: s(t) = n(t)$

Alternate hypothesis  $\mathcal{H}_1: s(t) = n(t) + h(t)$

Odds ratio:  $\mathcal{O} = \frac{P(\mathcal{H}_1|s(t))}{P(\mathcal{H}_0|s(t))}$ , further expanding by Bayes theorem:  $\mathcal{O} = \frac{P(\mathcal{H}_1)}{P(\mathcal{H}_0)} \frac{P(s(t)|\mathcal{H}_1)}{P(s(t)|\mathcal{H}_0)}$

Since the *prior odds*  $\frac{P(\mathcal{H}_1)}{P(\mathcal{H}_0)}$  is the *a priori* knowledge between the hypothesis, it is weighted with the *likelihood ratio* (Bayes factor)  $\frac{P(s(t)|\mathcal{H}_1)}{P(s(t)|\mathcal{H}_0)}$  which gives the *a posteriori* distribution of the data.

### Understanding the Matched Filter

$h(t) \rightarrow \tilde{h}(t)$  such that in time domain, a cross-correlation is done by multiplying and sliding monochromatic frequencies at every frequency and calculate the integral.

$$\mathcal{F}(h) := \tilde{h}(f) = \int_{-\infty}^{\infty} dt h(t) \exp(-\imath 2\pi f t)$$

*Sophisticated pattern matching!* Fourier transform is the simplest matched filter.

The convolution

$$s * h(\tau) = \int dt s(t)h(t + \tau)$$

evolves to a product in frequency domain as

$$\mathcal{F}(s * h(\tau)) = \tilde{s}(f) \cdot \tilde{h}(f)$$

Naively, we define the *naive* matched filter as

$$(s, h) = \int_0^{\infty} df \tilde{s}(f) \tilde{h}(f)$$

Leads to issues with normalization since the power is unbounded. Thereby, defining the matched-filter as

$$\frac{(s, h)}{\sqrt{(h, h)}} = \frac{\int_0^{\infty} df \tilde{s}(f) \tilde{h}(f)}{\sqrt{\int_0^{\infty} df \tilde{h}(f) \tilde{h}(f)}}$$

Discriminating power in understanding the phase modulation greater than the amplitude modulation.

### Noise weighted Inner-Product

Consider a zero-mean Gaussian noise, with variance  $\sigma^2$ , distributed as

$p_n(x_j) \propto \exp\left(-\frac{1}{2\sigma^2}x_j^2\right)$ , leading to the joint probability distribution

$$p_n[\{x_j\}] = \left(\frac{1}{\sqrt{2\pi}\sigma}\right)^N \exp\left[-\frac{1}{2\sigma^2} \sum_{j=0}^{N-1} x_j^2\right]$$

From the definition of the PSD, we have  $S_n(f) = \lim_{\Delta t \rightarrow 0} 2\sigma^2 \Delta t$ , such that

$$\lim_{\Delta t \rightarrow 0} \exp\left[-\frac{1}{2\sigma^2} \sum_{j=0}^{N-1} x_j^2\right] = \lim_{\Delta t \rightarrow 0} \exp\left[-\frac{1}{S_n(f)} \sum_{j=0}^{N-1} \langle x_j^2 \rangle\right]$$

This further simplifies to

$$\exp\left[-\int_{-\infty}^{\infty} \frac{[\tilde{x}(f)]^2}{S_n(f)}\right]$$

For colored noise, the time series is produced through a convolution of white noise

$$\gamma(t) = \int_{-\infty}^{\infty} K(t-t') x(t') dt'$$

which is a product in the frequency domain is  $\tilde{\gamma}(f) = \tilde{K}(f)\tilde{x}(f)$  thereby, defining the inner product as

$$(a, b) \equiv 4\Re \int_0^{\infty} \frac{a^*(f)b(f)}{S_n(f)}$$

we have the probability distribution as

$$p_n[s(t)] \propto \exp\left(-\frac{1}{2}(s, s)\right)$$

## Detection Statistics

The likelihood ratio is

$$\Lambda(\vec{\lambda}, \mathcal{H}_1 | s(t)) = \frac{p(s(t) | \vec{\lambda}, \mathcal{H}_1)}{p(s(t) | \mathcal{H}_0)}$$

where we marginalize over the parameter set  $\vec{\lambda}$ . The probability of the noise, assuming null hypothesis, is

$$p(s(t) | \mathcal{H}_0) = p_n[s(t)] \propto \exp(-\frac{1}{2}(s, s))$$

For the alternate hypothesis,

$$p(\vec{\lambda}, s(t) | \mathcal{H}_0) = p_n[s(t) - h(t; \vec{\lambda})] \propto \exp(-\frac{1}{2}(s - h, s - h))$$

Thereby, the likelihood ratio is

$$\Lambda(\vec{\lambda}, \mathcal{H}_1 | s(t)) = \exp(s, h) \exp(-\frac{1}{2}(h, h))$$

For normalization,

$$h(\vec{\lambda}) = \rho(\vec{\lambda}) \hat{h}(\vec{\lambda})$$

such that the *matched filter SNR*, normalizes  $\Lambda$  with  $\frac{d\Lambda}{d\rho} = 0$ , such that

$$\rho_{mf}(\vec{\lambda}) = (s, \hat{h}(\vec{\lambda})) = \frac{(s, h(\vec{\lambda}))}{\sqrt{(h(\vec{\lambda}), h(\vec{\lambda}))}}$$

with the ensemble average as the *optimal SNR* being

$$\langle \rho_{mf}(\vec{\lambda}) \rangle = \rho_{opt}(\vec{\lambda})$$

## Template Bank

We note that we can combine the extrinsic parameters to give an effective amplitude  $A$ , and further marginalize over the time and coalescence phase, hence dependence on intrinsic parameters.

- Analytic marginalization over extrinsic parameters such that

$$\frac{\partial \log \Lambda(\mathcal{H}_1 | s(t))}{\partial \vec{\lambda}} \Big|_{\vec{\lambda}=\vec{\lambda}_{\max}} \equiv \left[ (s, \hat{h}(\vec{\lambda})) - \frac{1}{2} (\hat{h}(\vec{\lambda}), \hat{h}(\vec{\lambda})) \right]_{\vec{\lambda}=\vec{\lambda}_{\max}} = 0$$

- Time marginalization through SNR timeseires and maximum value

Template bank  $h(t, \vec{\lambda}) = Ag(t - t_0, \vec{\lambda})$ , thereby

$$(s, h) = 2A \int_{-\infty}^{\infty} \frac{\tilde{s}(f) \tilde{g}^*(f)}{S_n(f)} \exp(i2\pi f t_0) df$$

Phase marginalization, with data  $\tilde{h}(f; \vec{\lambda}, \phi) \tilde{g}(f; \vec{\lambda}) \exp(i\phi_c)$ , with two templates at  $\phi_c = 0, \frac{\pi}{2}$ , such that

$$(s, h)_{\max} = \sqrt{(s, h(0))^2 + \left(s, h\left(\frac{\pi}{2}\right)\right)^2}$$

- For intrinsic parameters, we grid the continuous extrinsic parameter space with templates. fine-graining so that dense packing ensures template recovery.

Accuracy of template bank, characterized by fitting factor, and the fractional loss in SNR in nearby templates as

$$1 - (u(t, \vec{\lambda}_i), u(t, \vec{\lambda}_i + \Delta \vec{\lambda}_i)) = 1 - \mathcal{A}$$

where the *ambiguity factor* defined as

$$\mathcal{A} = 1 - \left( -\frac{1}{2} \left( u(t, \vec{\lambda}_i), \frac{\partial^2 u(t, \vec{\lambda}_i)}{\partial \lambda_i \partial \lambda_j} \right) \right) d\lambda_i d\lambda_j$$

such that we define an effective metric  $g_{ij} = -\frac{1}{2} \left( u(t, \vec{\lambda}_i), \frac{\partial^2 u(t, \vec{\lambda}_i)}{\partial \lambda_i \partial \lambda_j} \right)$  in the template bank space.

## Frequentist's Model Selection

Detection statistic results in a distribution due to noise, thereby defining a threshold for the detection statistic to compare between the hypotheses. *False alarm rate* for the null hypothesis above the threshold, and *false dismissal* when true hypothesis falls below the threshold. Aim is to refine the detection statistic to distinguish the overlaps.

*p-value* is thereby, the probability of obtaining results observed at least as extreme as the result actually observed. Integrating the true hypothesis from the threshold value to higher, resulting in a confidence.

For the null hypothesis

$$p(\rho_{mf} | \mathcal{H}_0) = \frac{1}{\sqrt{2\pi}} \exp \left( -\frac{1}{2} \rho_{mf}^2 \right)$$

and for the alternate hypothesis,

$$p(\rho_{mf} | \mathcal{H}_1) = \frac{1}{\sqrt{2\pi}} \exp \left( -\frac{1}{2} (\rho_{mf}^2 - \rho_{opt}^2) \right)$$

Analytically, the *false alarm rate* is related through the erf function.

## Coherent Tests

Since detectors are not co-located, or co-aligned, the non-Gaussian noises are local, hence coherent analysis can be done through

- $\chi^2$  test: Coherent power stream analysed.

Break the detector bandwidth into smaller bands and note if the response in each band is consistent with signal. The loss in SNR in bands is characterized by the difference of actual SNR in each bin subtracted from the total SNR weighted by number of bins:

$$\Delta\rho_j := \rho_j - \frac{\rho}{p}$$

We further define

$$\chi^2 := \chi^2(\rho_1, \dots, \rho_p) = p \sum_{j=1}^p (\Delta\rho_j)^2$$

such that the mean  $\langle \chi^2 \rangle = p - 1$ , which gives us the total degrees of freedom, due to the constraint of the total SNR.

Higher  $\chi^2$  results in lower probability of occurrence from a natural signal.

- Veto out: External study, to remove seismic noises.

We down-weight the samples where data does not appear Gaussian, by re-weighting the total SNR. Combining the SNR timeseries and the  $\chi_r^2$  series as

$$\chi_r^2 := \chi_r^2(\rho_1, \dots, \rho_p) = \frac{p}{2p-2} \sum_{j=i}^p (\Delta\rho_j)^2$$

as the effective SNR

$$\hat{\rho}(t) = \begin{cases} \frac{1}{\frac{1}{2}[1+(\chi_r^2(t))^3]^{\frac{1}{6}}} \rho(t) & \chi_r^2 \geq 1 \\ \rho(t) & \text{otherwise} \end{cases}$$

- Time Consistency Tests: Arrival time differences at each detectors based on source location and inter-detector baseline.  $\Delta t_{ij} = t_j - t_i = \frac{(\vec{r}_j - \vec{r}_i) \cdot \hat{n}}{c}$ . Re-binning the SNRs through time window sliding.
- Multi-Detector Coincidence: Triggers from multiple detectors checked for coincidence.
- Null Stream test: Construct linear combinations of data streams, to reveal glitches.

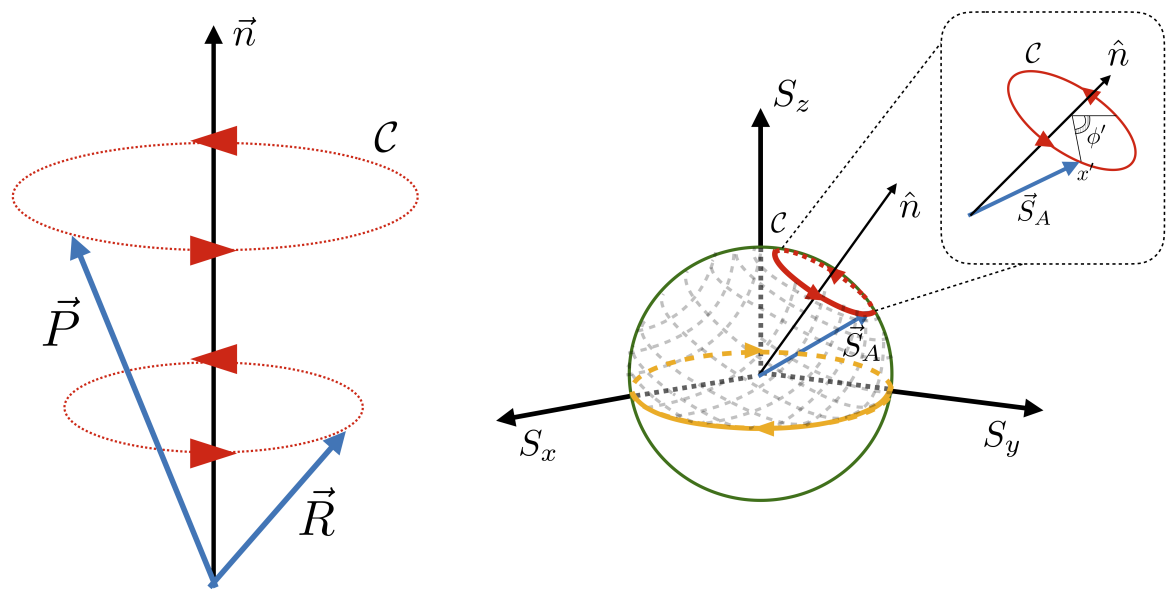
# 03.01 Estimation of GW Parameters

## Signal Morphology

$$h(t; \vec{\lambda}) = \sum_{i=+, \times} F_i(\alpha, \delta, \psi) h_i(t; \vec{\lambda})$$

Intrinsic Parameters:

- Masses ( $M_1, m_2$ )  
Higher mass, higher amplitude, shorter signal
- Spins ( $\vec{\chi}_1, \vec{\chi}_2$ )  
Aligned with orbital angular momentum, longer signal  
Precession results in amplitude modulation
- Tidal Deformabilities ( $\Lambda_1, \Lambda_2$ )  
For neutron stars, with tidal effects



Extrinsic Parameters:

- Luminosity distance  $d_L$   
Distance to the source defined by the relative flux
- Sky location  $(\alpha, \delta)$   
Relative position in the celestial sphere
- Polarization  $\psi$   
Affects the antenna pattern functions, angle of polarization
- Inclination angle  $\theta_{jn}$   
Relative orientation of the source

## Bayes Theorem

The *posterior* probability distribution is encompassed as

$$p(\vec{\lambda}|d, \mathcal{H}) = \frac{\mathcal{L}(d|\vec{\lambda})\pi(\vec{\lambda}|\mathcal{H})}{\mathcal{Z}}$$

where *Likelihood*  $\mathcal{L}$  is the probability of the noise residual

$$\mathcal{L}(d|\vec{\lambda}) = \prod_i \frac{2}{T} \frac{1}{S_n(f_i)} \exp \left[ -\frac{2}{T} \frac{1}{S_n(f)} (d - h(\vec{\lambda}))^2 \right]$$

and the corresponding *prior*  $\pi$  encompassing the distributions for masses (uniform, uniform in  $\mathcal{M}, q$ ), spins (Isotropic), sky location, inclination angle, luminosity distance  $d_L$  (Power law). The *evidence*  $\mathcal{Z}$  used for model selection serves as a normalization constant

$$\mathcal{Z} = \int \mathcal{L}(d|\vec{\lambda})\pi(\vec{\lambda}|\mathcal{H}) d\vec{\lambda}$$

with the ratio of evidences defined as the Bayes factor as

$$\mathcal{B} = \frac{Z_1}{Z_0} = \frac{\int \mathcal{L}(d|\vec{\lambda})\pi(\vec{\lambda}|\mathcal{H}_1) d\vec{\lambda}}{\int \mathcal{L}(d|\vec{\lambda})\pi(\vec{\lambda}|\mathcal{H}_0) d\vec{\lambda}}$$

## Marginalizing the Posterior

Integrating the *nuisance* parameters, resulting in a marginalized posterior

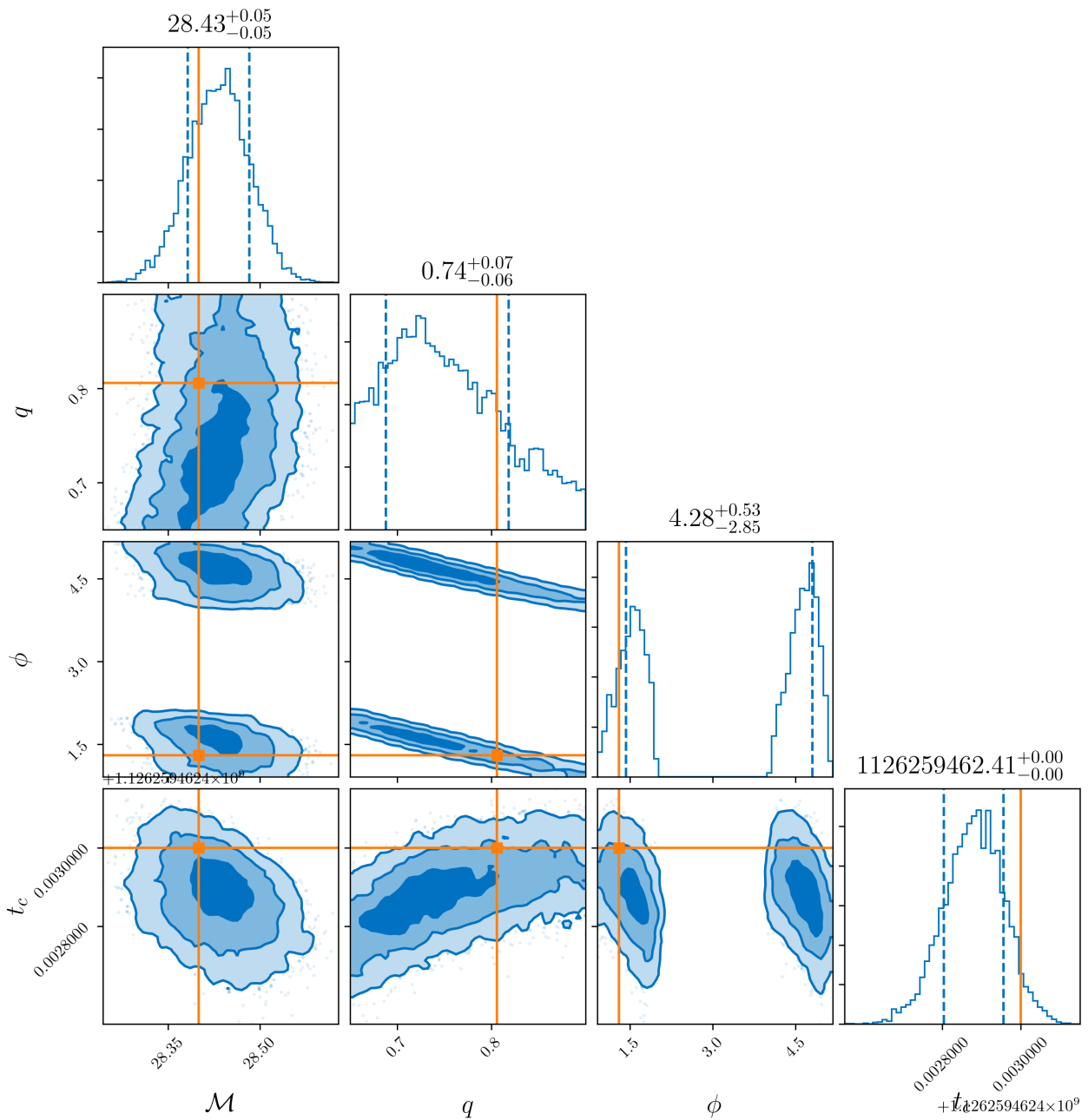
$$p(\lambda_i|d) = \int \left( \prod_{k \neq i} d\theta_k \right) p(\vec{\lambda}|d) = \frac{\mathcal{L}(d|\lambda_i)\pi(\lambda_i|\mathcal{H})}{\mathcal{Z}}$$

where the marginalized likelihood is

$$\mathcal{L}(d|\lambda_i) = \int \left( \prod_{k \neq i} d\theta_k \right) \mathcal{L}(d|\vec{\lambda})$$

## Parameter Estimation

The priors from the samples are updated every iteration through the Bayes theorem to obtain the posteriors



Posteriors are sampled through a *MCMC* (Monte Carlo Markov Chain) Sampling. Simpler through *Rejection Sampling*, wherein a proxy distribution is used to sample  $x$  and  $u \in \mathcal{U}(0, 1)$  and check if  $u \leq \frac{f(x)}{Cg(x)}$ , such that the point is in the curve and repeat. But, higher rejection rates and non-efficient.

Monte Carlo estimate uses randomness to sample points to set up a Markov chain of transient estimates. The probability of jumping from one state to another depends *only* on the current states, described the transition matrix, resulting in a *memoryless* process. It exhibits a *stationery state* distribution, such that  $pT = p$ , to obtain a fixed distribution. We design the Markov chain such that the stationery distribution is the target distribution such that  $p(x_0)T(x_1|x_0) = p(x_1)T(x_0|x_1)$ .

### ② Metropolis-Hastings MCMC Algorithm >

- Trial sample  $x_t = x_n + \delta$

- Compute acceptance probability  $P_a = \min\left(\frac{p(x_t)}{p(x_n)}, 1\right)$
- Draw  $r \in \mathcal{U}(0, 1)$ , accept if  $r < P_a$ , else reject
- $x_{n+1} = \begin{cases} x_n & r < P_a \\ x_t & r > P_a \end{cases}$

Nested Sampling involves expressing the evidence

$$\mathcal{Z} = \int \mathcal{L}(d|\theta) \pi(\theta) d\theta = \int \mathcal{L}(X) dX$$

where

$$X(\Lambda) = \int_{\mathcal{L}(\vec{\lambda}) > \Lambda} \pi(\vec{\lambda}) d\vec{\lambda}$$

giving the effective prior mass. Iteratively, the prior mass is reduced, with rejecting samples with low likelihood. Larger samples in region of likelihood.

- Start with random samples  $\vec{\lambda}_1, \dots, \vec{\lambda}_n$ , setting  $\mathcal{Z} = 0$ , with  $X_0 = 1$  as the highest prior mass
- Find the lowest  $\mathcal{Z}$  from the  $n$  points, and set  $X_1 = \exp(-\frac{1}{N})$  and sample.
- Update the evidence as  $\mathcal{Z} \rightarrow \mathcal{Z} + \mathcal{Z}(X_0 - X_1)$
- Repeat above steps such that  $X_i = \exp(-\frac{i}{N})$  and  $\mathcal{Z} \rightarrow \mathcal{Z} + \mathcal{Z}(X_i - X_{i-1})$
- After  $j$  steps, we have the evidence  $\mathcal{Z} \rightarrow \mathcal{Z} + \frac{1}{N}[\mathcal{Z}(\lambda_0) + \dots + \mathcal{Z}(\lambda_n)]$